Chinese Journal of Natural Medicines

Repurposing diacerein to suppress colorectal cancer growth by inhibiting the DCLK1/STAT3 signaling pathway

Qiaobei YE, Yu ZHU, Meng SHI, Linxi LV, Yuyan GONG, Luyao ZHANG, Lehe YANG, Haiyang ZHAO, Chengguang ZHAO, Huanhai XU

Citation: Qiaobei YE, Yu ZHU, Meng SHI, Linxi LV, Yuyan GONG, Luyao ZHANG, Lehe YANG, Haiyang ZHAO, Chengguang ZHAO, Huanhai XU, Repurposing diacerein to suppress colorectal cancer growth by inhibiting the DCLK1/STAT3 signaling pathway, Chinese Journal of Natural Medicines, 2024, 22(4), 318−328. doi: 10.1016/S1875−5364(24)60621−7.

View online: https://doi.org/10.1016/S1875−5364(24)60621−7

Available online at www.sciencedirect.com
ScienceDirect
Chinese Journal of Natural Medicines 2024, **22**(4): 318-328
doi: 10.1016/S1875-5364(24)60621-7
Chinese Journal of Natural Medicines

•Original article•

Repurposing diacerein to suppress colorectal cancer growth by inhibiting the DCLK1/STAT3 signaling pathway

YE Qiaobei[1Δ], ZHU Yu[1, 2, 3Δ], SHI Meng[1, 2, 3Δ], LV Linxi[1, 2, 3], GONG Yuyan[1, 2, 3], ZHANG Luyao[1], YANG Lehe[1], ZHAO Haiyang[2*], ZHAO Chengguang[1, 2, 3*], XU Huanhai[1*]

[1] *Affiliated Yueqing Hospital, Wenzhou Medical University, Wenzhou 325600, China;*
[2] *The Institute of Life Sciences, Biomedical Collaborative Innovation Center of Zhejiang Province, Wenzhou University, Wenzhou 325035, China;*
[3] *School of Pharmaceutical Sciences, Wenzhou Medical University, Wenzhou 325035, China*

Available online 20 Apr., 2024

[ABSTRACT] Double cortin-like kinase 1 (DCLK1) exhibits high expression levels across various cancers, notably in human colorectal cancer (CRC). Diacerein, a clinically approved interleukin (IL)-1β inhibitor for osteoarthritis treatment, was evaluated for its impact on CRC proliferation and migration, alongside its underlying mechanisms, through both *in vitro* and *in vivo* analyses. The study employed MTT assay, colony formation, wound healing, transwell assays, flow cytometry, and Hoechst 33342 staining to assess cell proliferation, migration, and apoptosis. Additionally, proteome microarray assay and western blotting analyses were conducted to elucidate diacerein's specific mechanism of action. Our findings indicate that diacerein significantly inhibits DCLK1-dependent CRC growth *in vitro* and *in vivo*. Through high-throughput proteomics microarray and molecular docking studies, we identified that diacerein directly interacts with DCLK1. Mechanistically, the suppression of p-STAT3 expression following DCLK1 inhibition by diacerein or specific DCLK1 siRNA was observed. Furthermore, diacerein effectively disrupted the DCLK1/STAT3 signaling pathway and its downstream targets, including MCL-1, VEGF, and survivin, thereby inhibiting CRC progression in a mouse model, thereby inhibiting CRC progression in a mouse model.

[KEY WORDS] DCLK1; Diacerein; Rhein; STAT3; Colorectal cancer
[CLC Number] R965 **[Document code]** A **[Article ID]** 2095-6975(2024)04-0318-11

Introduction

Colorectal cancer (CRC) ranks as the second most common cause of cancer-related mortality worldwide [1]. Although advances in early diagnosis through sophisticated screening technologies and novel treatment approaches have significantly enhanced the overall survival rate of CRC patients over the past few decades, approximately half of these patients experience local or distant relapse after conventional treatment [2]. Consequently, research efforts have been directed toward identifying sensitive biomarkers and developing innovative therapies for CRC.

Double cortin-like kinase 1 (DCLK1), belonging to both the protein kinase superfamily and the doublecortin family, exhibits aberrant expression in several human cancers, including those of the colorectum, kidney, and pancreas [2-4]. The overexpression of DCLK1 is closely associated with advanced tumor stages, metastasis, and reduced survival rates in CRC patients [5]. Moreover, DCLK1 serves as a biomarker for pinpointing patients at high risk and those with tumors resistant to chemotherapy [5, 6]. Therefore, the creation of DCLK1-specific medications represents a promising strategy for CRC treatment.

Diacerein has been shown to possess anti-inflammatory, analgesic, and antipyretic properties [7]. Additionally, it is prescribed clinically prescribed for patients suffering from osteoarthritis. In humans, diacerein is fully metabolized into rhein. In this study, we evaluated the therapeutic effects of di-

[Received on] 12-Jul.-2023
[Research funding] This work was supported by the National Natural Science Foundation of China (Nos. 82173856 and 82203322), the Natural Science Foundation of Zhejiang Province (Nos. LY21H300005 and LGF22H030014), Wenzhou Municipal Science and Technology Bureau (Nos. ZY2020025 and H20210009), and the Science and Technology Innovation Activity Plan for College Students of Zhejiang Province (No. 2019R413012).
[*]**Corresponding author]** E-mails: 20160106@wzu.edu.cn (ZHAO Haiyang); zhaochengguang@wmu.edu.cn (ZHAO Chengguang); xhh19992000@163.com (XU Huanhai)
[Δ]These authors contributed equally to this work.
These authors have no conflict of interest to declare.

acerein both *in vitro* and *in vivo*. Through human proteome microarray and molecular docking analyses, we explored diacerein's influence on the DCLK1/signal transducer and activator of transcription 3 (STAT3) signaling pathway. Collectively, our results suggest that DCLK1 represents a viable target for CRC treatment, and diacerein emerges as a novel DCLK1 inhibitor in the realm of anti-tumor therapy.

Materials and Methods

Patient tissues

Nine pairs of human CRC tissues and adjacent normal tissues were collected from the First Affiliated Hospital of Wenzhou Medical University. The clinicopathological details of all the specimens are outlined in Supplementary File 1. These fresh tissues were promptly snap-frozen and preserved at −80 °C. The study received ethical approval from the Ethics Committee of the First Affiliated Hospital of Wenzhou Medical University, and written informed consent was obtained from all participating patients.

Cell culture

The human CRC cell lines human colon carcinoma cell line HCT116, RKO, SW480 and DLD-1 were acquired from the Shanghai Institute of Biosciences and Cell Resources Center, Shanghai, China. The HCT116 cells were cultured in McCoy's 5A medium, while the SW480, RKO, and DLD-1 cells were maintained in the RPMI 1640 medium. All media were enriched with 10% fetal bovine serum (FBS) and 1% penicillin/streptomycin. The cells were incubated in a humidified atmosphere at 37 °C with 5% CO_2.

Antibodies and reagents

The antibodies against VEGF, survivin, MCL-1, DCLK1, STAT3, and GAPDH were purchased from Cell Signaling Technology (Danvers, MA, USA). Antibodies against Cl-caspase 3, BAX, and p-STAT3 were purchased from Abcam (Cambridge, UK). Antibodies against BCL2, HRP-conjugated goat anti-mouse IgG, and horseradish peroxidase (HRP)-conjugated donkey anti-rabbit IgG were purchased from Santa Cruz Biotechnology (Santa Cruz, CA, USA). Dia was procured from Aladdin Biochemical Technology (Shanghai, China). Dimethyl sulfoxide (DMSO) and MTT were purchased from Sigma-Aldrich (St. Louis, MO, USA). The Annexin V-FITC Apoptosis Detection Kit I was purchased from BD Pharmingen (Franklin Lakes, NJ, USA).

MTT cytotoxicity assay

Cells (5×10^3 cells/well) were plated in 96-well plates and cultured overnight. After a 48-h incubation period with the drug, 25 μL of MTT solution was added to each well for 4 h. Next, the formazan crystals were solubilized in 150 μL of DMSO, and the optical density was measured at 490 nm by a microplate reader. The half-maximal inhibitory concentration (IC_{50}) was calculated using GraphPad Pro Prism 7.0 software (GraphPad, San Diego, CA).

Colony formation assay

CRC cells, at a density of $1–1.5 \times 10^3$ cells/well, were seeded in 6-well plates and incubated overnight. The medium was then supplemented with DMSO (control) and various concentrations of diacerein. The culture medium was refreshed every two days over a period of 1–2 weeks. Subsequently, colonies were fixed with 4% paraformaldehyde for 10 min, rinsed 2–3 times with phosphate-buffered saline (PBS), and stained with crystal violet for 10 min.

Wound healing migration assay

RKO cells were cultured in 6-well plates until they reached 80%–90% confluence. Wounds were then created using a 10-μL pipet tip. Detached cells were removed by washing with PBS, and the adherent cells were treated with diacerein at concentrations of 30, 60, and 100 μmol·L^{-1} for 72 h in serum-free medium. The wounds were photographed at 0 and 72 h using a light microscope (Leica, Wentzler, Germany).

Transwell invasion assay

DLD-1 cells, at a density of 8×10^4 cells/well, were seeded into the upper chamber of Matrigel-coated Transwell inserts with serum-free medium and incubated overnight. Medium containing specified concentrations of diacerein (30, 60, and 100 μmol·L^{-1}) along with 20% FBS was added into the lower chamber of the Transwell inserts. After a 24-hour incubation period, the cells were fixed with 4% paraformaldehyde and stained with a crystal violet solution. The migrated cells were then photographed using a light microscope.

Flow cytometry analysis

CRC cells were seeded in 6-well plates and incubated overnight. Subsequently, they were treated with DMSO (serving as a control) or varying concentrations of diacerein (30, 60, 100 μmol·L^{-1}) for 48 h. Following the treatment period, the cells were harvested and stained with annexin V and propidium iodide PI as per the manufacturer's protocol. The fluorescence signal was then quantified using a FACS Calibur instrument (BD Biosciences; Baltimore, MD, USA).

Lactate dehydrogenase (LDH) assay

CRC cells were seeded in 96-well culture plates overnight and subsequently treated with DMSO (serving as the control) or diacerein at concentrations of 30, 60, 100 μmol·L^{-1} for 48 h. After this treatment period, positive drugs were added to the wells and incubated for an additional hour. The supernatant was then transferred to a new 96-well plate, to which LDH detection reagent was added, followed by incubation for 1h. The absorbance was measured at 490 nm. The LDH Cytotoxicity Assay Kit utilized in this procedure was sourced from the Beyotime Institute of Biotechnology.

Hoechst 33342 staining

The morphological characteristics of the apoptotic cells were observed using a Hoechst 33342 Assay Kit from the Beyotime Institute of Biotechnology, China. HCT116 and RKO cells were seeded in 6-well plates and treated with DMSO (as control) or diacerein at concentrations of 30, 60, and 100 μmol·L^{-1} for 48 h. Subsequently, the cells were fixed with 4% paraformaldehyde for 15 min and stained with Hoechst 33342 solution for 20 min. The stained cells were then visualized and photographed using a fluorescent microscope.

Western blotting analysis

Proteins were extracted from both cells and tissues using lysis buffer, then separated by Sodium dodecyl-sulfate polyacrylamide gel electrophoresis (SDS-PAGE) using either 10% or 12% gels and subsequently transferred to PVDF membranes. The membranes were blocked with 5% skim milk for 1.5 h at room temperature. Primary antibodies were applied and incubated overnight at 4°C, followed by the application of HRP-conjugated secondary antibodies for 1 h at room temperature. Immunoreactive bands were visualized using the Bio-Rad ChemiDoc XRS chemiluminescence imaging system (Bio-Rad Laboratories, Hercules, CA, USA).

Synthesis of biotinylated rhein

To synthesize the intermediate 2, 878 mg (6.5 mmol) of HOBt, 500 mg (6.5 mmol) of EDCI, 1.22 g (5 mmol) of D-biotin, and 30 mL of DMF were combined in a 100-mL vial, stirred until dissolved. Subsequently, 1.2 g (20 mmol) of ethylenediamine and *N*, *N*-diisopropylethylamine (DIPEA) were added under an argon atmosphere and stirred at room temperature overnight. Following the reaction's completion, as indicated by TLC, the mixture was concentrated under reduced pressure and purified *via* a column to obtain intermediate 2 (280 mg; yield, 10%).

Next, 68 mg (0.5 mmol) of HOBt, 96 mg (0.5 mmol) of EDCI, 57 mg (0.2 mmol) of rhein, and 3 mL of DMF were added into a 100-mL vial and stirred until dissolved. Intermediate 2 (57 mg, 0.2 mmol) and DIPEA (129 mg, 1 mmol) were then introduced under an argon atmosphere and stirred at room temperature overnight. Upon verifying the reaction's completion *via* TLC, 10 mL of water was added to precipitate the solid, which was then filtered, washed with water, and further purified with dichloromethane. After filtration, the product was obtained (20 mg; yield, 20%).

Proteome microarray assay

The Arrayit HuProt v2.0 19K Human Proteome Microarray (CDI Laboratories, Baltimore, MD) underwent a blocking process with 3% Bovine Serum Albumin (BSA) at room temperature for 1 h. Subsequently, after dilution to 10 μmol·L^{-1} in blocking buffer, the microarray was treated with biotinylated-rhein, also at room temperature for 1 h, followed by incubation with Cy3-streptavidin (diluted 1 ∶ 1000, Sigma-Aldrich) for another hour at the same temperature. After these steps, the microarray was dried and then scanned using the GenePix 4200A microarray scanner (Molecular Devices, San Jose, CA, USA). Data analysis was performed with GenePix Pro 6.0 software, where the signal-to-noise ratio (SNR) was calculated as the difference between the median foreground and median background values. An SNR cutoff value was established at > 1.1 for significant binding events.

Molecular docking

Molecular docking was conducted utilizing AutoDock Vina 1.0.2 software. The crystal structure of DCLK1, identified by the PDB code 5JZJ, was obtained from Protein Data Bank. Input files for both the ligand and the receptor were prepared using AutoDock Tools version 1.5.6, provided by The Scripps Research Institute, CA, USA. In the docking procedure, the protein was treated as a rigid body, whereas the ligand was allowed flexibility.

siRNA transfection

Specific siRNA oligonucleotides targeting DCLK1 were designed and procured from Genepharma, Shanghai, China. The sequences for the siRNA primers were as follows: siDCLK1-1 (5'-CCAGUCCCAUGCUGUACAATT-3'), siDCLK1-2 (5'-GGGUUUACCAUCAAGAGAUTT-3'), and siDCLK1-3 (5'-GGAUAAGACCACCGCUCUUTT-3'). For transfection, cells were treated with 50 nmol·L^{-1} siRNA employing Lipofectamine 3000 (Invitrogen, Waltham, MA, USA) and incubated for 48 h.

In vivo tumor xenograft mouse model

The animal studies were conducted at Wenzhou Medical University with the approval of its Animal Care and Use Committee. Female athymic BALB/c nude mice aged 5–6 weeks were purchased from the Vital River Experimental Animal Center, Beijing, China. HCT116 cells were injected into the hind flanks of the mice under anesthesia with isoflurane. Upon the tumors reaching a volume of 50 mm^3, the mice were randomly divided into three groups (n = 5). The groups received intraperitoneal injections of diacerein at doses of 30 mg·kg^{-1} every two days or 60 mg·kg^{-1} every two days or PBS as a control. The tumor volume was calculated using the formula: 0.5 × length × width^2. Measurements of tumor volumes and mouse body weights were taken bi-daily. Following a 14-day period, the mice were euthanized, and the tumors were excised for subsequent immunohistochemistry and western blot analyses. Additionally, the livers, kidneys, hearts, and lungs were collected for hematoxylin–eosin staining.

Immunohistochemistry staining

Tumor tissues were fixed in 10% paraformaldehyde solution and subsequently embedded in paraffin. The paraffin-embedded tissues were then sectioned into 5-μm-thick slices. Following this preparation, the sections were incubated with an anti-DCLK1 primary antibody overnight at 4 °C. An appropriate secondary antibody was applied for signal detection. Afterward, the sections underwent staining with diaminobenzidine (DAB) and were counterstained with hematoxylin for nuclei visualization. Images of the stained sections were captured using a light microscope.

SPR analysis

The Surface Plasmon Resonance (SPR) analysis was conducted following the OpenSPR™ instrument's standard operating procedures for installing the NTA chip. The procedure began by running the assay buffer, PBS, at the maximum flow rate of 150 μL·min^{-1}. After achieving a stable signal baseline, the flow rate was adjusted to 20 μL·min^{-1}. The chip surface was functionalized by injecting a prepared solution of imidazole and $NiCl_2$ through the inlet port. For the analysis, 200 μL of solubilized ligand protein was prepared and introduced at a flow rate of 20 μL·min^{-1} for a binding duration of 4 min. The stability of the baseline was monitored for 5 min to ensure consistency. Upon stabilization of the ligand signal, a high concentration of the analyte was injected to verify the activity of the ligand and to estimate the surface's maximum

binding capacity approximately. The chip was then regenerated by increasing the flow rate to 150 μL/min and injecting the chosen regeneration buffer to effectively remove the analyte.

The analyte was diluted with buffer and introduced at a flow rate of 30 μL·min^{-1}. The binding interaction between the protein and ligand lasted for 60 s, followed by a natural dissociation period of 120 s. GraphPad Prism7 software, utilizing the Steady State Affinity analysis model, was employed to analyze the results.

Statistical analysis

Kaplan–Meier survival curve analysis was conducted using the KMplot program (http://kmplot.com/analysis/). Data from non-animal experiments were presented as mean ± SD of three independent experiments. For animal studies, statistical analysis involved data from at least eight animals per group. Comparison between different groups was performed using Student's t-test or one-way analysis of variance. A *P*-value ≤ 0.05 was deemed to indicate statistical significance.

Results

Diacerein inhibits human CRC cell proliferation, invasion, and migration

The MTT assay was utilized to evaluate cell viability following treatment with diacerein (Fig. 1A). The findings demonstrated that diacerein significantly reduced the viability of CRC cells in a dose-dependent manner. Specifically, the IC_{50} values for diacerein were found to be 46.56 ± 2.848 μmol·L^{-1} in HCT116 cells, 29.93 ± 2.155 μmol·L^{-1} in RKO cells, 33.47 ± 8.498 μmol·L^{-1} in SW480 cells, and 53.55 ± 1.458 μmol·L^{-1} in DLD-1 cells (Fig. 1B). Additionally, colony formation assays indicated that diacerein effectively inhibited the formation of cell colonies in a dose-dependent manner (Fig. 1C). Moreover, wound-healing and Transwell assays demonstrated that diacerein significantly reduced CRC cell invasion and migration, also in a dose-dependent fashion (Figs. 1D and 1E).

Diacerein induces apoptosis in human CRC cells

To investigate the induction of apoptosis by diacerein in human CRC cells, three cancer cell lines were treated with diacerein for 48 h and subsequently stained with Annexin V and PI for apoptosis analysis. The rate of apoptosis was assessed using flow cytometry. The findings indicated that diacerein prompted apoptosis in a dose-dependent manner (Fig. 2A). Additionally, the morphological features of the apoptotic cells were observed through Hoechst 33342 staining, corroborating the dose-dependent effect of diacerein on inducing apoptosis (Fig. 2B). Western blotting analysis further supported these results, revealing an increase in the expression levels of bcl-2-like protein 4 (BAX) and Cl-Caspase 3, alongside a decrease in BCL-2 expression (Fig. 2C). Moreover, it was demonstrated that diacerein does not cause cell necrosis at the same concentrations (Fig. S1).

Proteomic identification of rhein-binding proteins and molecular docking studies

To elucidate the mechanism underlying diacerein's action, efforts were made to identify its potential binding proteins. Biotinylated rhein (bio-rhein) was synthesized (Fig. 3A and Supplementary File 2). The MTT assay was employed to evaluate the viability of CRC cells, aiming to compare the inhibitory effects of both diacerein and synthesized bio-rhein. The IC_{50} value of bio-rhein in HCT116 cells was determined to be 51.65 μmol·L^{-1}, closely aligning with diacerein's approximated IC_{50} value of 46.56 μmol·L^{-1} (Fig. 3B). A human proteomic microarray, encompassing approximately 75% of the human proteome with 19 394 purified GST-tagged proteins, was used for screening. The microarray, hybridized with bio-rhein, identified binding interactions *via* Cy3-conjugated streptavidin (Cy3-SA), calculating the signal-to-noise ratio (SNR) for each spot. The screening pinpointed four proteins that interacted with bio-rhein, among which DCLK1 demonstrated the strongest binding affinity (Fig. 3C). Molecular docking simulations further indicated that diacerein targets the ATP-binding site of DCLK1, establishing five hydrogen bonds with specific residues (ILE396, VAL468, ASP472, LYS419 and ASP533) (Fig. 3D). SPR analysis corroborated the binding affinity of diacerein to DCLK1 across varying concentrations (Fig. S2), suggesting its potential role as an ATP-competitive inhibitor of DCLK1. Collectively, these findings, derived from proteomic microarray and molecular docking analyses, support the hypothesis that DCLK1 is a direct target of diacerein.

Diacerein inhibits the DCLK1 signaling pathway in human CRC cells

The study investigated the suppressive effects of diacerein on DCLK1 in human CRC cells. Through Western blotting analysis, it was observed that diacerein notably decreased DCLK1 levels in a dose-dependent manner (Fig. 4A). Meanwhile, diacerein down-regulated STAT3 phosphorylation in HCT116, RKO, and DLD-1 cells without altering the expression levels of total STAT3. Furthermore, diacerein also diminished the expression of STAT3 target proteins, namely MCL-1, VEGF, and survivin (Fig. 4A). To explore the role of DCLK1 in CRC cells, treatments with siRNA-control or siRNA-DCLK1 were conducted, followed by Western blotting analysis. The results demonstrated that the knockdown of DCLK1 significantly decreased the levels of both DCLK1 and phosphorylated STAT3 in CRC cells (Figs. 4B and 4C). To substantiate diacerein's inhibitory impact on cell proliferation and ascertain the critical role of DCLK1 in this process, the viability of HCT116 and RKO cells, either depleted of DCLK1 or not, was assessed post-diacerein treatment. The MTT assay revealed that diacerein exerted negligible effects on cells with DCLK1 knockdown (Fig. 4D).

Diacerein inhibits tumor growth in the xenograft mouse model

Building on the *in vitro* cytotoxicity findings associated with diacerein, its therapeutic efficacy was further assessed in an HCT116 xenograft mouse model. Mice were administered intraperitoneal injections of diacerein at doses of 30 mg·kg^{-1} every two days or 60 mg·kg^{-1} every two days, with PBS

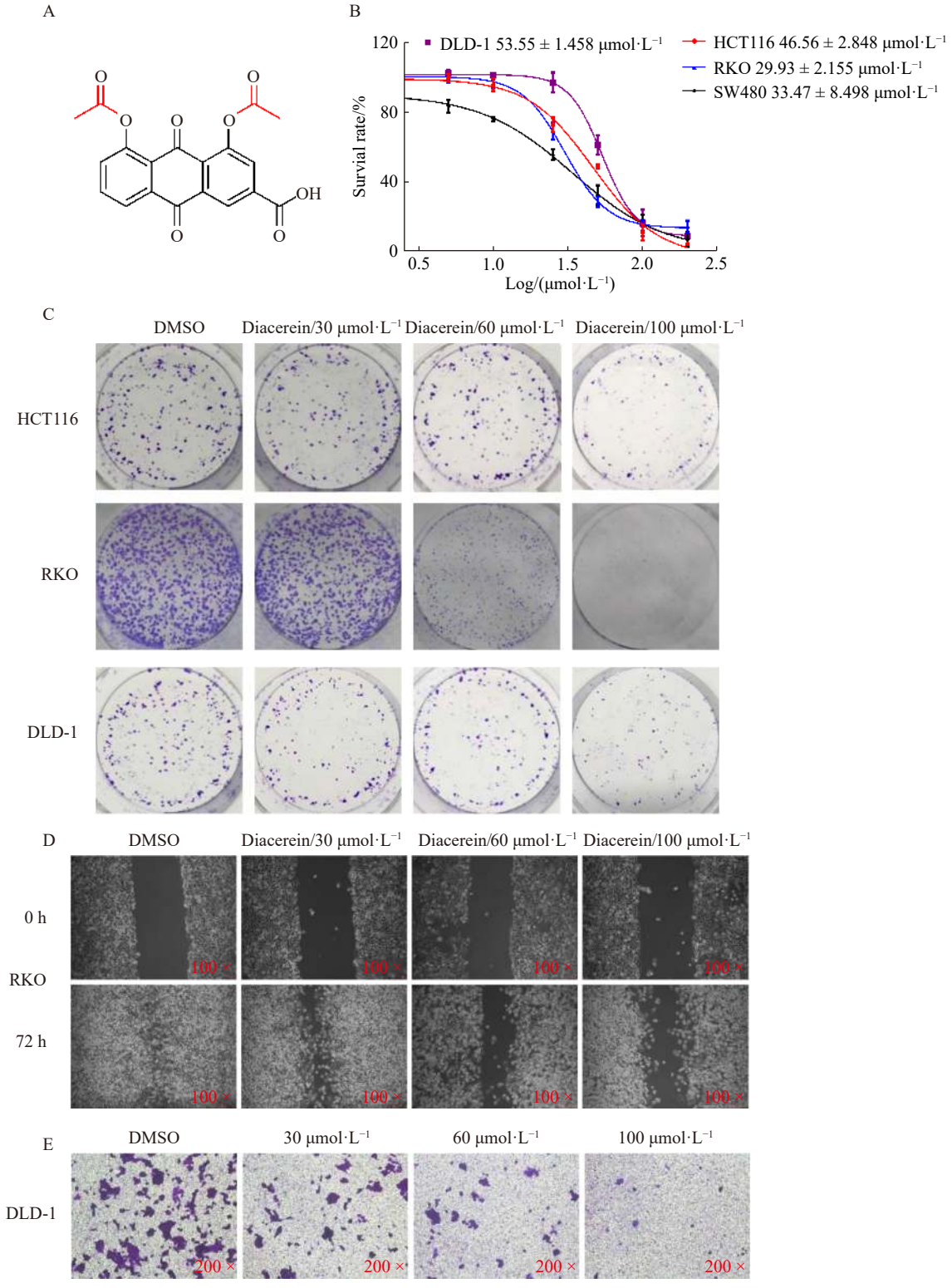

Fig. 1 Diacerein inhibits CRC cell proliferation and migration. (A) Chemical structure of diacerein (Rhein acid is esterified to form diacerein, and the red part in the figure shows the changed structure). (B) CRC cell viability assessed by MTT assay after diacerein treatment for 48 h, and the IC_{50} value is indicated. (C) CRC cells are incubated in a diacerein-containing medium for 24 h and allowed to form colonies for 1–2 weeks. (D) RKO cells are plated in 6-well plates for 24 h, then scratched and exposed to diacerein for 72 h and observed microscopically (100× magnification). (E) CRC cells are seeded in Transwell upper chambers and treated with diacerein for 24 h. The migrating cell number is determined (200× magnification).

serving as the control. The body weight of the mice and the volume of the tumors were measured bi-daily. Results demonstrated that both the volume and weight of tumors in the diacerein-treated groups were significantly lower compared to the control group (Figs. 5A–5C). No major difference in the body weight was observed among the three groups (Fig. 5D), indicating that the treatment did not adversely affect the overall health of the mice. Further analysis through hematoxylin-eosin staining revealed no significant cytotoxic damage to the kidneys, heart, liver, and lungs across all groups (Fig. 5F), suggesting that diacerein was well-tolerated at the administered doses. A notable finding was the observed down-regulation of DCLK1 expression in the diacerein-treated groups (Fig. 5E), reinforcing the hypothesis that DCLK1 is a primary target of diacerein *in vivo*. Collectively, these results underscore diacerein's potential as an effective anti-CRC drug candidate, chiefly through the inhibition of the DCLK1/STAT3 signaling pathway.

DCLK1 is highly expressed in human CRC tissues

Kaplan–Meier survival curve analysis revealed a significant inverse relationship between the level of DCLK1 protein in tumor specimens and the survival duration of CRC patients, with a *P*-value of 0.032) (Fig. 6A). This suggests that higher DCLK1 expression in tumors is associated with shorter survival times. To further investigate DCLK1's role in CRC, Western blotting and immunofluorescence staining were conducted to assess the protein levels of DCLK1 in human CRC tissues as well as in adjacent normal tissues. The results from western blot analysis demonstrated an increase in DCLK1 expression in 6 out of 9 (66.67%) tumor tissues when compared to their adjacent normal tissues (Fig. 6B). These findings were corroborated by immunohistochemistry

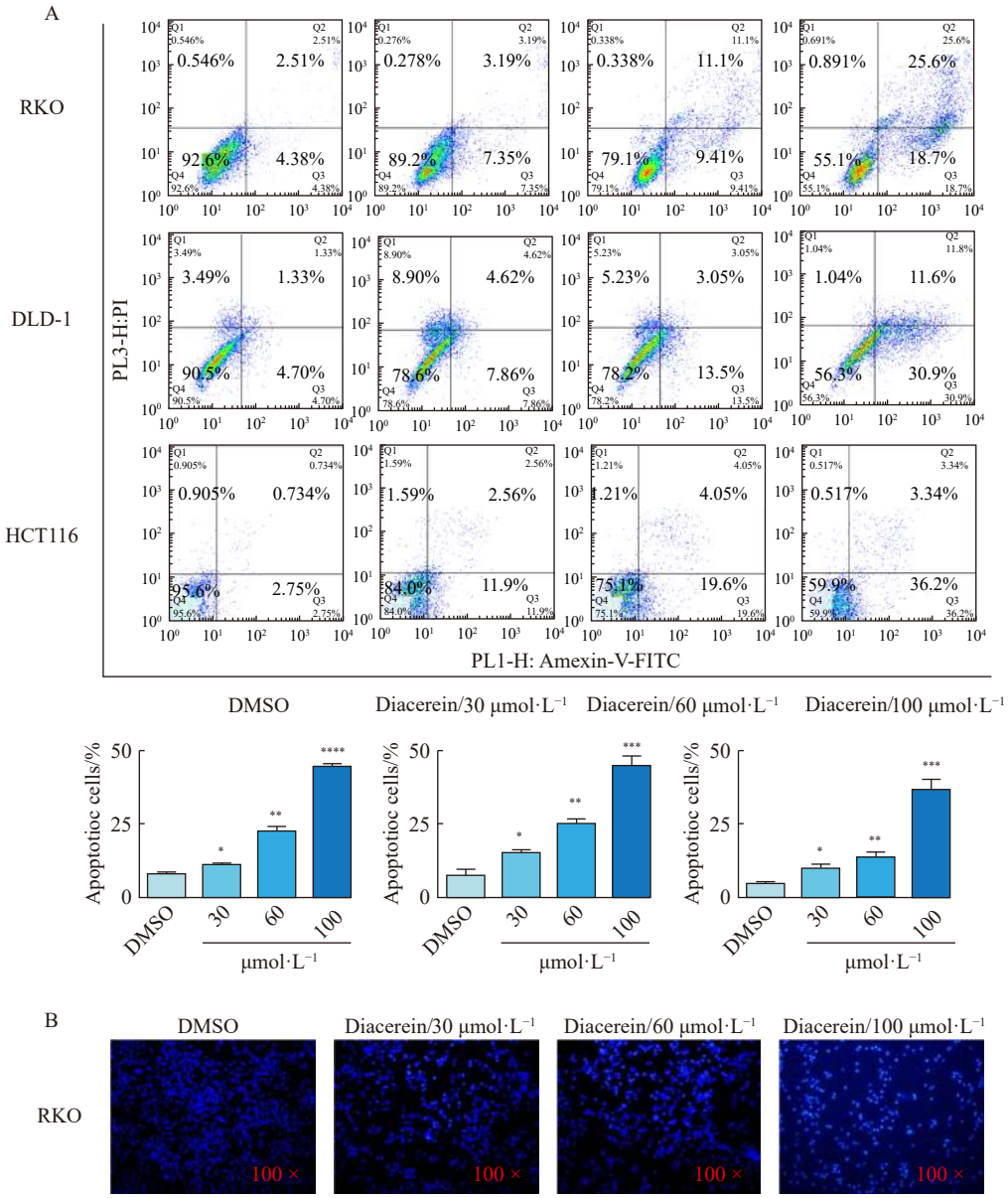

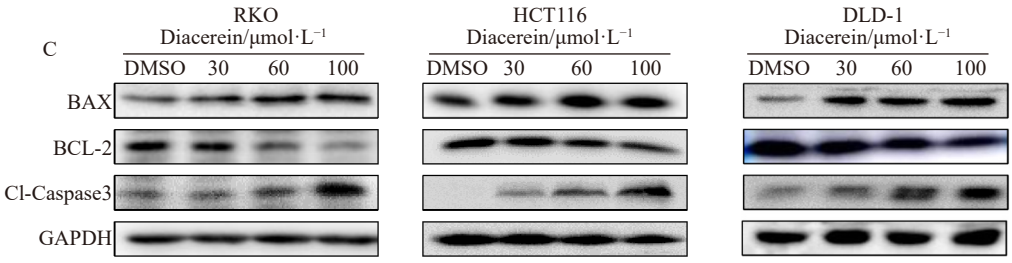

Fig. 2 Diacerein induces apoptosis in CRC cells. (A) After 48 h of diacerein treatment, RKO, HCT116, and DLD-1 cells are collected, and apoptotic cells are analyzed by flow cytometry. Statistical analysis of the percentage of apoptotic cells is shown. (B) RKO cells are stained with Hoechst 33342 and observed under a fluorescence microscope (100× magnification). (C) The expressions of BCL2, BAX, and Cl-Caspase3 in RKO, HCT116, and DLD-1 cells after 24 h of treatment with diacerein are measured *via* Western blotting assays.

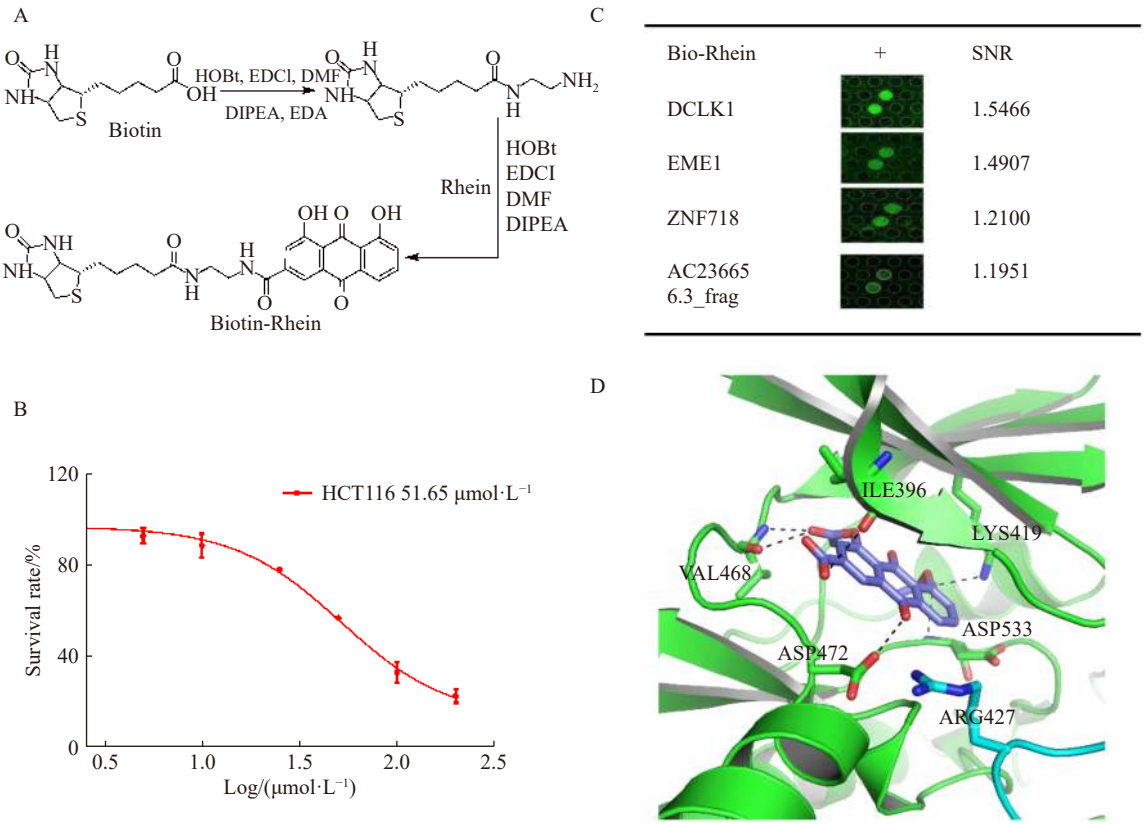

Fig. 3 Proteomic identification of diacerein-binding proteins and molecular docking. (A) Chemical structure of biotin-labeled rhein (bio-rhein). (B) MTT assay determines the viability of HCT116 cells exposed to biotin-labeled rhein. (C) Enlarged image of bio-rhein binding to recombinant DCLK1 protein spots on the microarray, and the calculated signal-to-noise ratio. (D) Molecular docking of diacerein binding to DCLK1 crystal structure.

analysis, which provided additional verification of DCLK1's elevated expression in tumor tissues (Fig. 6C). The collective evidence from these analyses suggests that DCLK1 could potentially act as a biomarker for the diagnosis of CRC.

Discussion

DCLK1 is notably overexpressed in CRC and other solid tumors, where it is associated with heightened metastasis and adverse patient prognoses [4]. DCLK1 is implicated in modulating pro-survival and self-renewal signaling pathways within intestinal tumor cells [8]. Despite its significance, the repertoire of inhibitors targeting DCLK1 remains limited. To date, only three inhibitors—Leucine-rich repeat kinase 2 IN-1 (LRRK2-IN-1), NVP-TAE684, and XMD8-92—have been documented to curtail tumor growth in CRC and pancreatic cancer xenograft models by aiming at DCLK1 [9]. However, these inhibitors exhibit low specificity for DCLK1 and concurrently inhibit other kinases, including leucine-rich repeat kinase 2 (LRRK2), mitogen-activated protein kinase 7 (MAPK7), and anaplastic lymphoma kinase (ALK), respectively [10-12]. Given the high attrition rates of drug candidates during the discovery phase and the objective to minimize de-

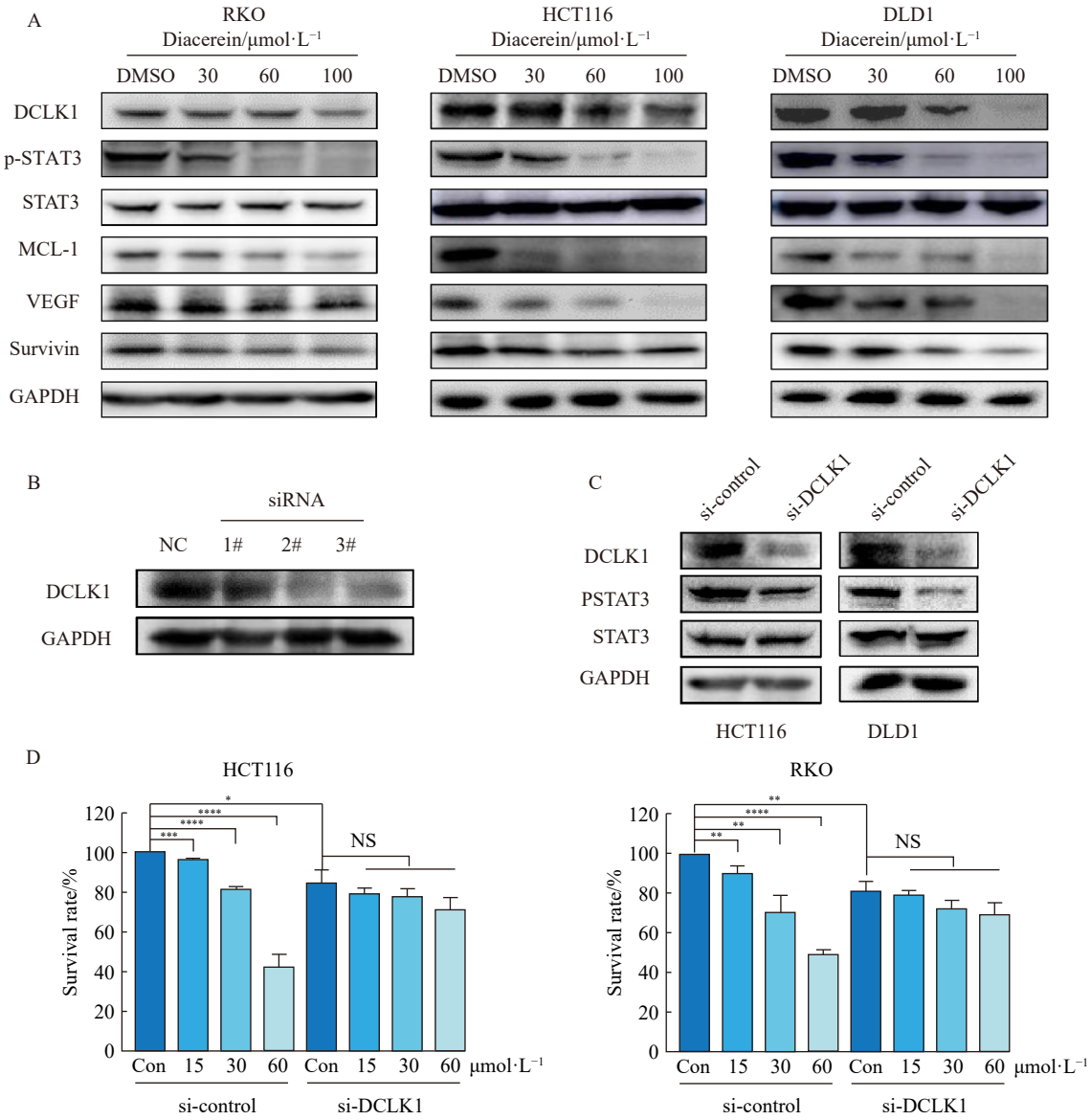

Fig. 4 Diacerein inhibits the DCLK1 signaling pathway in CRC cells. (A) Western blotting assay quantifies the levels of DCLK1/STAT3 pathway-related proteins in CRC cells treated with diacerein for 24 h. (B) DCLK1 protein level after HCT116 cells are transfected with DCLK1 siRNA (named as si1, si2, and si3) for 48 h. (C) Western blotting assay quantifies the levels of DCLK1 and STAT3 in HCT116 and DLD-1 cells transfected with DCLK1 siRNA2. (D) The survival rate of HCT116 and RKO cells transfected with si-control or si-DCLK1 and treated with diacerein for 48 h. $^{*}P < 0.05$, $^{**}P < 0.01$, $^{***}P < 0.001$, $^{****}P < 0.0001$.

velopment costs and timeframes, leveraging existing drugs to identify new small-molecule inhibitors for DCLK1 presents a strategic and efficient approach. For instance, niclosamide, an FDA-approved anthelmintic drug, has been identified as a potent inhibitor of DCLK1 [2].

In this study, we demonstrated that diacerein effectively inhibited tumor growth in both CRC cell lines and a xenograft mouse model. STAT3 emerges as a promising target for cancer therapy due to its critical role in various biological processes, including cell proliferation, angiogenesis, metastasis, and maintaining stem cell-like properties [13]. Our findings suggest that DCLK1 modulates STAT3 signaling in CRC, positioning DCLK1 as a potential biomarker for therapies targeting STAT3 (Fig. 7). Interestingly, diacerein has previously been shown to exert anti-tumorigenic effects in breast cancer, attributed to its ability to dampen IL6/STAT3 signaling [7, 14]. This aligns with our previous research, which highlighted the anti-tumor properties of various natural products, including corylin, through their targeting of the STAT3 pathway [15]. Moreover, the interaction between STAT3 and other signaling molecules is increasingly recognized as vital in the development of effective cancer therapies [16, 17], underscoring the importance of a nuanced understanding of these pathways in the fight against cancer.

Diacerein, currently approved for osteoarthritis-treatment, operates through the modulation of inflammatory

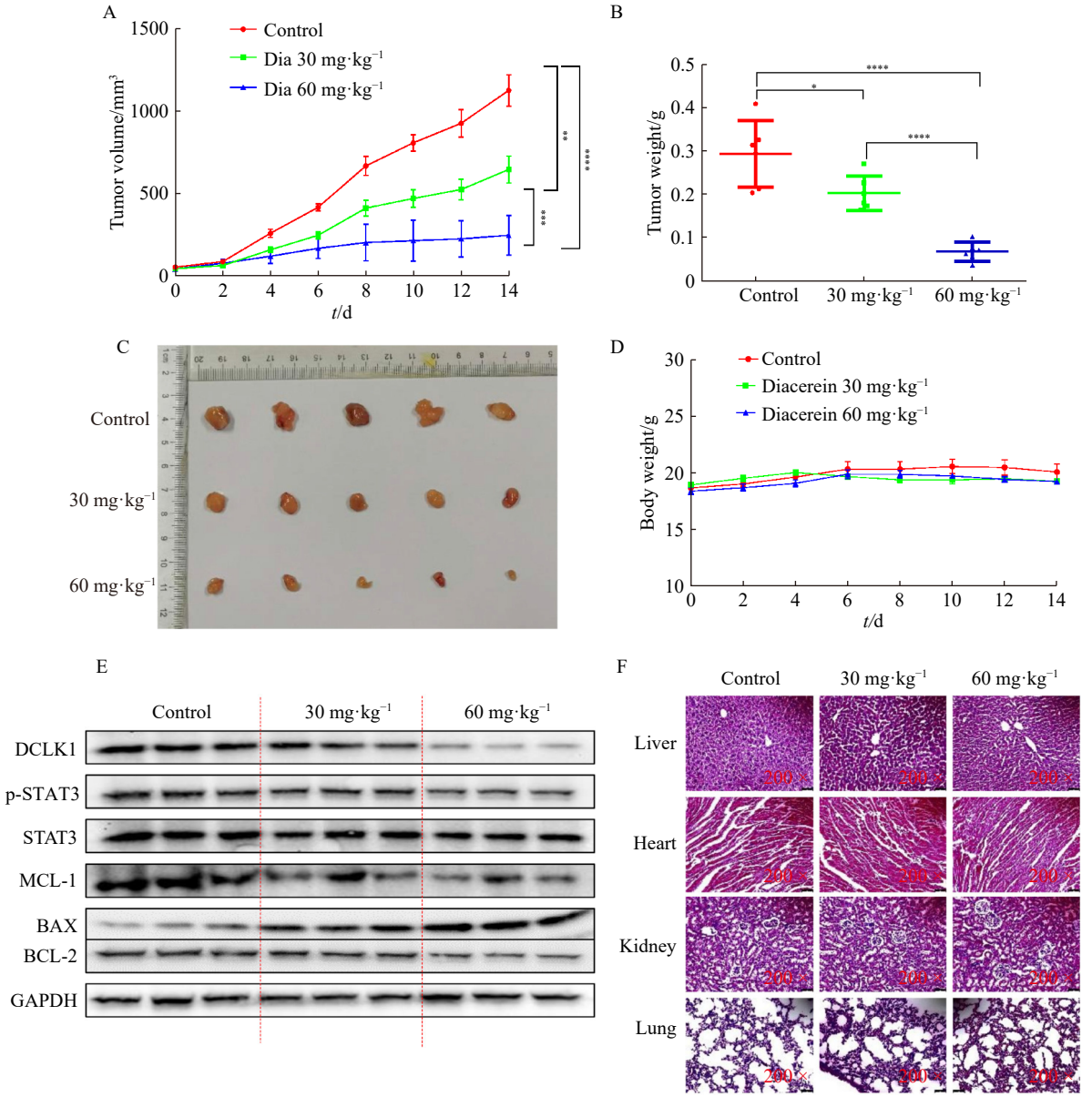

Fig. 5 Diacerein inhibits the growth of CRC xenograft model. (A, B) Tumor volume and tumor mass in nude mice treated with diacerein or PBS. (C) The appearance of tumors isolated from the mouse xenograft model. (D) Body weight curves of nude mice treated with diacerein or PBS. (E) The levels of DCLK1/STAT3 pathway-associated proteins and apoptosis-related proteins in tumor tissue were monitored by western blot analysis. (F) Representative photomicrographs of sections of livers, hearts, lungs, and kidneys in nude mice (200 × magnification).

cytokines [18] and is safely metabolized into rhein in humans [19]. This study has illuminated diacerein's potential efficacy and safety in CRC therapy by targeting the DCLK1/STAT3 signaling pathway. However, the clinical application of diacerein for CRC treatment faces challenges due to its low solubility and permeability, slow dissolution rate, and suboptimal bioavailability [20]. To address these limitations and enhance the therapeutic potential of diacerein (or rhein) in CRC [14], further research involving advanced drug delivery systems is warranted. Such investigations could significantly improve the bioavailability and clinical viability of diacerein, paving the way for its repositioning as a beneficial agent in cancer therapy.

Conclusions

Leveraging diacerein's ability to inhibit STAT3 activators, which are known to facilitate the growth of CRC, our findings offer a persuasive rationale for repurposing diacerein as a potentially innovative therapeutic option for CRC.

Supplementary Materials

Supplementary data to this article can be obtained by sending an E-mail to the corresponding authors.

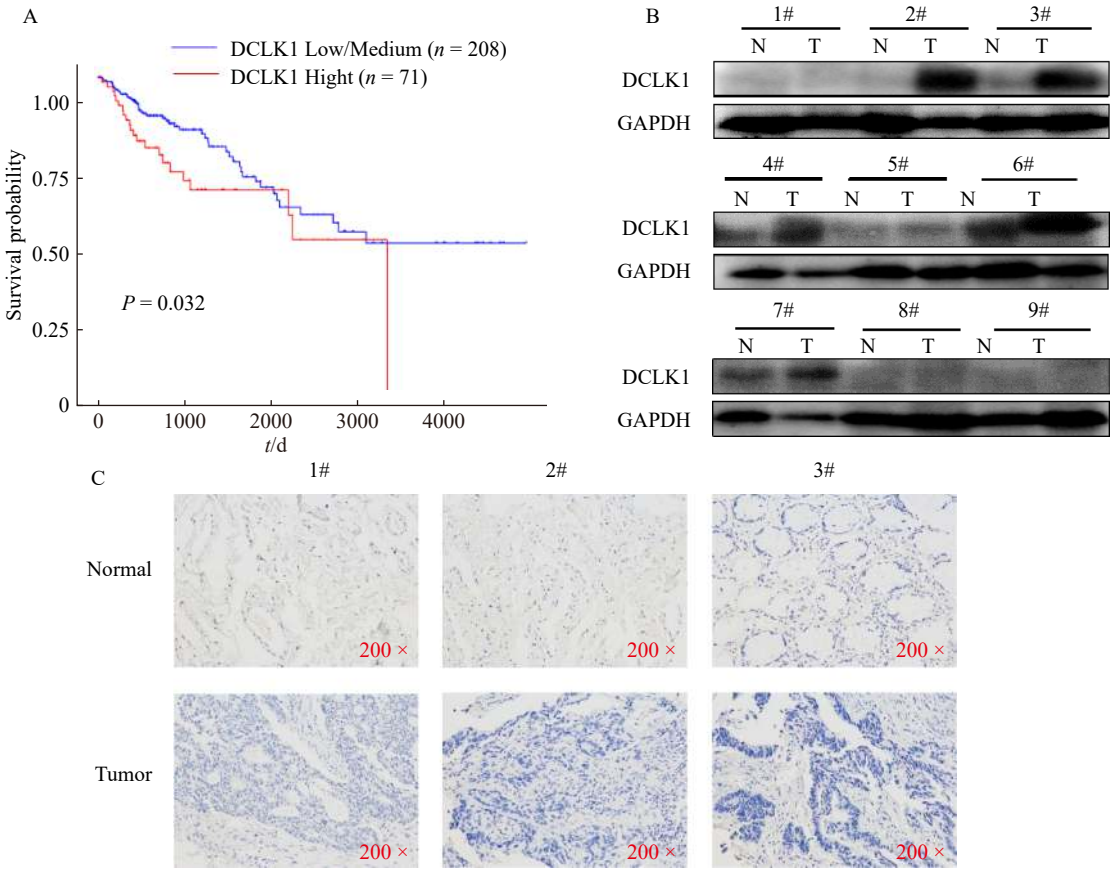

Fig. 6 DCLK1 is highly expressed in human colonic carcinoma tissues. (A) Kaplan–Meier survival analysis. (B) Protein level of DCLK1 in CRC tissue samples (T) and adjacent normal colonic tissues (N) obtained from the different patients. (C) Immunohistochemistry analysis of DCLK1 in CRC tissue and normal tissue samples (200 × magnification).

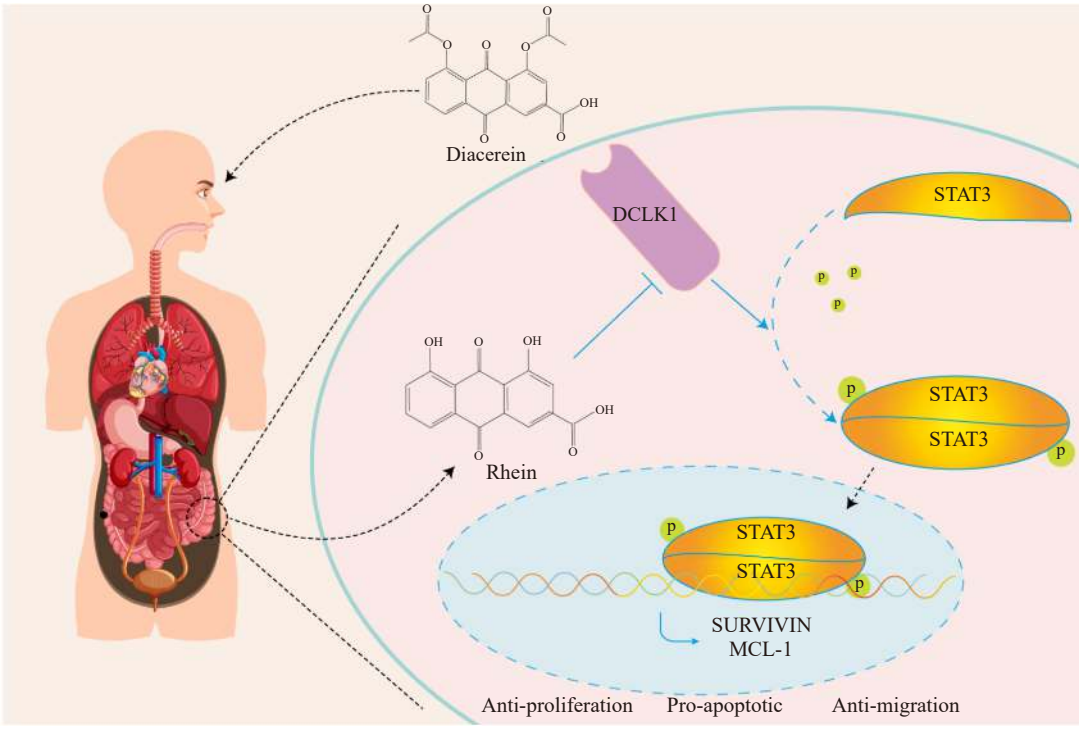

Fig. 7 Diacerein serves as a new DCLK1 inhibitor. Diacerein is metabolized into rhein in the body, which is targeted to inhibit the DCLK1/STAT3 signaling pathway to exert anti-colorectal cancer activity.

Ethics Approval and Consent to Participate

All patients provided written informed consent to participate. The study was conducted according to international guidelines and approved by the Ethics Committee of the Affiliated Yueqing Hospital of Wenzhou Medical University (approval number: YS2019-424). All animal procedures were approved by Wenzhou Medical University Animal Policy and Welfare Committee (approval number: wydw-2020-0320). All patients provided written informed consent.

References

[1] Sung H, Ferlay J, Siegel RL, *et al*. Global cancer statistics 2020: GLOBOCAN estimates of incidence and mortality worldwide for 36 cancers in 185 countries [J]. *CA Cancer J Clin*, 2021, **71**(3): 209-249.

[2] Park SY, Kim JY, Choi JH, *et al*. Inhibition of lEF1-mediated DCLK1 by niclosamide attenuates colorectal cancer stemness [J]. *Clin Cancer Res*, 2019, **25**(4): 1415-1429.

[3] Nakanishi Y, Seno H, Fukuoka A, *et al*. Dclk1 distinguishes between tumor and normal stem cells in the intestine [J]. *Nat Genet*, 2013, **45**(1): 98-103.

[4] Qiu W, Remotti HE, Tang SM, *et al*. Pancreatic DCLK1^{+} cells originate distinctly from PDX1^{+} progenitors and contribute to the initiation of intraductal papillary mucinous neoplasm in mice [J]. *Cancer Lett*, 2018, **423**: 71-79.

[5] Gzil A, Szylberg Ł, Jaworski D, *et al*. The essential role of DCLK1 in pathogenesis, diagnostic procedures and prognostic stratification of colorectal cancer [J]. *Anticancer Res*, 2019, **39**(6): 2689-2697.

[6] Nguyen CB, Kotturi H, Waris G, *et al*. (*Z*)-3,5,4'-Trimethoxystilbene limits hepatitis C and cancer pathophysiology by blocking microtubule dynamics and cell-cycle progression [J]. *Cancer Res*, 2016, **76**(16): 4887-4896.

[7] Bharti R, Dey G, Ojha PK, *et al*. Diacerein-mediated inhibition of IL-6/IL-6R signaling induces apoptotic effects on breast cancer [J]. *Oncogene*, 2016, **35**(30): 3965-3975.

[8] Chandrakesan P, Yao J, Qu D, *et al*. Dclk1, a tumor stem cell marker, regulates pro-survival signaling and self-renewal of intestinal tumor cells [J]. *Mol Cancer*, 2017, **16**(1): 30.

[9] Patel O, Dai W, Mentzel M, *et al*. Biochemical and structural insights into doublecortin-like kinase domain 1 [J]. *Structure*, 2016, **24**(9): 1550-1561.

[10] Weygant N, Qu D, Berry WL, *et al*. Small molecule kinase inhibitor LRRK2-IN-1 demonstrates potent activity against colorectal and pancreatic cancer through inhibition of doublecortin-like kinase 1 [J]. *Mol Cancer*, 2014, **13**: 103.

[11] Sureban SM, May R, Weygant N, *et al*. XMD8-92 inhibits pancreatic tumor xenograft growth *via* a DCLK1-dependent mechanism [J]. *Cancer Lett*, 2014, **351**(1): 151-161.

[12] Galkin AV, Melnick JS, Kim S, *et al*. Identification of NVP-TAE684, a potent, selective, and efficacious inhibitor of NPM-ALK [J]. *Proc Natl Acad Sci USA*, 2007, **104**(1): 270-275.

[13] Johnson DE, O'keefe RA, Grandis JR. Targeting the IL-6/JAK/STAT3 signalling axis in cancer [J]. *Nat Rev Clin Oncol*, 2018, **15**(4): 234-248.

[14] Bharti R, Dey G, Banerjee I, *et al*. Somatostatin receptor targeted liposomes with Diacerein inhibit IL-6 for breast cancer therapy [J]. *Cancer Lett*, 2017, **388**: 292-302.

[15] Yang L, Yao Y, Bai Y, *et al*. Effect of the isoflavone corylin from *Cullen corylifolium* on colorectal cancer growth, by targeting the STAT3 signaling pathway [J]. *Phytomedicine*, 2021, **80**: 153366.

[16] Yang L, Zhou F, Zhuang Y, *et al*. Acetyl-bufalin shows potent efficacy against non-small-cell lung cancer by targeting the CDK9/STAT3 signalling pathway [J]. *Br J Cancer*, 2021, **124**(3): 645-657.

[17] Yang L, Lin S, Kang Y, *et al*. Rhein sensitizes human pancreatic cancer cells to EGFR inhibitors by inhibiting STAT3 pathway [J]. *J Exp Clin Cancer Res*, 2019, **38**(1): 31.

[18] Fidelix TS, Macedo CR, Maxwell LJ, *et al*. Diacerein for osteoarthritis [J]. *Cochrane Database Syst Rev*, 2014, (2): CD005117.

[19] Yang L, Li J, Xu L, *et al*. Rhein shows potent efficacy against non-small-cell lung cancer through inhibiting the STAT3 pathway [J]. *Cancer Manag Res*, 2019, **11**: 1167-1176.

[20] Eltobshi AA, Mohamed EA, Abdelghani GM, *et al*. Self-nanoemulsifying drug-delivery systems for potentiated anti-inflammatory activity of diacerein [J]. *Int J Nanomedicine*, 2018, **13**: 6585-6602.

Cite this article as: YE Qiaobei, ZHU Yu, SHI Meng, LV Linxi, GONG Yuyan, ZHANG Luyao, YANG Lehe, ZHAO Haiyang, ZHAO Chengguang, XU Huanhai. Repurposing diacerein to suppress colorectal cancer growth by inhibiting the DCLK1/STAT3 signaling pathway [J]. *Chin J Nat Med*, 2024, **22**(4): 318-328.